IEEE Access
Multidisciplinary | Rapid Review | Open Access Journal

Received April 22, 2021, accepted May 6, 2021, date of publication May 14, 2021, date of current version May 27, 2021.

Digital Object Identifier 10.1109/ACCESS.2021.3080297

An Intelligent System for Improving Electric Discharge Machining Efficiency Using Artificial Neural Network and Adaptive Control of Debris Removal Operations

CHENG-HSIUNG LEE AND TON-SHIN LAI
Master Program of Digital Innovation, Tunghai University, Taichung 40704, Taiwan
Corresponding author: Cheng-Hsiung Lee (hsiung@thu.edu.tw)

ABSTRACT Electrical discharge machining (EDM) can effectively solve the shortcomings of traditional machining processes that cannot process special materials, so it is widely used on workpieces with strong hardness materials, such as titanium alloys and tool steels to produce various molds and dies. However, the operating procedures of EDM are quite complicated and low machining productivity. To improve machining efficiency, this study develops an intelligent system that adaptively controls debris removal operations instead of using preset debris removal parameters. A feature extraction method is proposed in this study to effectively identify the machining states from streaming images of the machining curve for evaluating the appropriate time of the debris removal operation. Then, the extracted features feed into the artificial neural network model to establish a debris removal predicted model. The preliminary experimental result shows that the established predicted model can achieve an accuracy of 96.93% for a testing dataset containing 750 machining curve images. To further verify the effectiveness of the proposed intelligent system in improving EDM efficiency, we integrate the debris removal predicted model into the EDM machine and test it on the manufacturing site. Compared with the preset debris removal parameter, the proposed intelligent system can save nearly 38.60% of machining time for the machining depth of 6.45mm under specific EDM conditions.

INDEX TERMS Artificial intelligence, debris removal operation, electric discharge machining, intelligent system, machining efficiency.

I. INTRODUCTION

Electrical discharge machining (EDM) is one of the most widely used non-conventional material removal processes in manufacturing. It is extensively used on workpieces with strong hardness materials to produce various shapes of molds and dies [1]–[3]. The basis of the EDM process is to remove material from the part by performing a series of repeated discharges between a tool called electrode and the workpiece in the presence of a dielectric fluid [4], [5]. During the EDM process, the electrode and the workpiece need to be separated by a certain distance (known as the sparking gap) to facilitate the sparking. Since EDM does not make direct contact between the electrode and the workpiece, it can eliminate mechanical stresses, chatter, and vibration problems during machining [1], [3]. As the times evolve, several EDM variations such as wire-cut EDM, micro-EDM, and die-sinking EDM have emerged in the industry to cope with the machining of exotic materials or super hard metal alloys used exclusively to manufacture aeronautical and aerospace parts [1].

EDM has always been regarded as a difficult traditional topic in the manufacturing industry because the operation procedures of EDM are quite complicated and the slower material removal rate (MRR) [4]. Related studies aim to develop technological solutions to allow the EDM operators to quickly determine the optimal machining parameters to improve machining productivity on the various performance measures, such as MRR, surface quality, and machining time. The commonly used machining parameters in EDM can

The associate editor coordinating the review of this manuscript and approving it for publication was Mehdi Hosseinzadeh.

be broadly divided into two categories: namely electronic and non-electronic parameters [1], [3]. At present, many researchers have deeply explored the influence of electric parameters such as current, voltage, pulse on and off-time, etc., on improving the EDM efficiency [6]–[10]. Fenggou and Dayong [7] had developed an intelligent system to automatically determine and optimize the processing parameters in the die-sinking EDM process with artificial neural networks (ANN). It showed that taking the current peak value as the core feature is quite adequate and can achieve a good machining speed under the premise of guaranteeing processing accuracy. Salonitis *et al.* [8] simulated the die-sinking EDM process by the proposed a theoretical thermal model. The proposed model's predicted results concluded that the increase of the discharge current, the arc voltage, or the spark duration results in higher MRR and coarser workpiece surfaces. Joshi and Pande [9] proposed an intelligent model for the EDM process using the finite-element method (FEM) and ANN. An ANN model was designed to establish a relation between input machining conditions such as discharge power and spark on time and the machining performance measures such as MRR and tool wear rate (TWR). The current and the pulse off-time are the most significant machining parameter for MRR in stainless steel from the investigation of Rajmohan *et al.* [10]. But there is related research also reported that an increase in pulse off-time does not affect MRR and surface roughness (SR).

Besides electrical parameters, non-electrical parameters such as the flushing of dielectric fluid, influence of different types of dielectrics, vibration integration with the workpiece and electrode, and the electrode jump height also play a critical role in delivering optimal performance measures [1]. Due to the vibration assisted conventional EDM process can greatly improve the efficiency of process, this topic has been attracting the attention of researchers [11], [12]. Nguyen and Pham [12] has been made on Taguchi based single-objective optimization of vibration assisted die-sinking electrical discharge machining process while machining SKD61 die steel. In their experimental investigation, it has been found that MRR has been significantly improved by vibration operations into the workpiece. Dielectric fluids play an extremely important role in productivity, cost and quality of processed parts during EDM process. Wang *et al.* [13] conducted a comparative study on the performance of composite dielectrics, kerosene and distilled water, and reported that MRR and SR performed better when machining titanium alloys with composite dielectrics. Sadagopan and Mouliprasanth [5] investigated the effect of using different dielectrics, such as, biodiesel, transformer oil and kerosene on the material removal rate, electrode wear and surface roughness in EDM based on Taguchi's design of experiments. They found that biodiesel can be used as a dielectric in EDM. It gives high MRR and less electrode wear rate (EWR) when compared to the widely used kerosene dielectric. The accumulation of debris in the machining gap results in poor performance of EDM because it will cause carbon deposition phenomena and accumulate and connect between the electrode and the workpiece, which can easily lead to instability in the machining process, thereby affecting the machining quality and MRR [14].

Debris removal operations are a critical measure of improving the carbon deposition phenomena in EDM. When performing debris removal operation, the electrode tool will be raised (electrode jump) to increase the spark gap to make the dielectric current have enough space to remove the debris [15]. Most scholars currently focus on observing the influence of electrode jump height on the machining gap's debris movement using numerical simulation to obtain good machining stability [16]–[19]. Centin *et al.* [16] analyzed the dielectric fluid flow and the debris distribution in the machining gap during low and high electrode jumps using a computational fluid dynamics (CFD) simulation program. Their study showed that electrode jump height affected the wall concavity of holes in deep EDM. Wang and Han [18] proposed a three-dimensional simulation model of the flow field with liquid, gas, and solid phases for machining gap in electrode jump to analyze the mechanisms of debris and bubble movement. Although debris removal operations are necessary operations to maintain the EDM stability, electrode jump will reduce the machining efficiency because almost no material is removed during this period. To improve the EDM efficiency, Wang and Jia [19] determine optimal electrode jump height and electrode machining time by a simulation model of the gap flow field and voltage and current signals between electrode and workpiece in EDM. Experimental shows that the established model of simulating the gap flow field can accurately calculate the optimal electrode jump height.

Besides the electrode jump height, the number of debris removal operations is also closely related to the machining efficiency due to the more frequent debris removal operation, the less work time (during the discharge between the electrode and the workpiece). An EDM operator at the manufacturing site usually uses the preset debris removal parameters provided by the operating specifications to perform debris removal operations automatically. However, this way often causes lowers machining efficiency. Because even if the amount of accumulated debris is within the normal range, the debris removal operations still are executed regularly. If the debris removal operation can be carried out only when needed, it will promote machining efficiency obviously. To enable the EDM machine to have an intellectual ability that controls the debris removal operation adaptively, this study attempts to develop an intelligent system using artificial intelligence (AI) and computer vision technologies to show that effective control of debris removal operations can significantly improve machining efficiency. No previous research is dedicated to controlling the debris removal operations adaptively to improve machining efficiency based on our investigation. Therefore, our research results can provide an essential reference for related researches on improving EDM efficiency.

TABLE 1. Review the related researches of EDM that used non-electronic parameters in the past 5 years.

No.	Authors	Types of non-electronic parameters								Categories of methods	Year
		Electrode vibration	Workpiece vibration	Ultrasonic vibration	Dielectric type	Spark gap	Electrode jump height	Electrode machining time	Debris removal operation		
1	Mastud et al. [23]	✓								Simulation analysis	2015
2	Zhu et al. [24]		✓							Orthogonal experiment	2018
3	Liu et al. [25]			✓						Simulation analysis	2018
4	Wang et al. [19]						✓	✓		Numerical calculations	2018
5	Hanif et al. [22]				✓	✓				Statistical analysis	2019
6	Nguyen & Pham [12]		✓							Parameter optimization	2021
7	Our method								✓	Process monitoring and control	

The remainder of this paper is organized as follows. Related research work about EDM in recent years is described in Section 2. Section 3 presents the proposed the intelligent improving EDM efficiency system. Section 4 describes the classification method used in this study, and experimental results and discussion and conclusions are presented in Section 5 and in Section 6, respectively.

II. LITERATURE REVIEW

The principle basis of the electric discharge machine can be traced back to 1770, an English chemist, Dr. Joseph Priestly, discovered the continuous erosive results obtained from the sparks series. Until 1943, Dr. B.R. Lazarenko and Dr. N.I. Lazarenko of Moscow University used the destructive properties of electrical discharge to machining difficult-to-process metals. In 1950, Lazarenko developed an EDM system that used a resistance-capacitance type of power supply and later served as the conventional EDM prototype. In 1980, the United States invented a computer-aided EDM called the computer numerical controlled EDM. Since then, the EDM machining process has attracted worldwide attention [1], [20].

Since the thermal energy required by the EDM process is generated through the applied electrical energy, the electrical parameters are crucial in improving the efficiency of electrical discharge machining [21]. In addition to the various electrical factors, non-electronic parameters are also needed much attention for the EDM process [22]. Table 1 summarizes the recent papers published in EDM-based work using various types of non-electronic parameters. This research differs from scholars in recent years in selecting non-electric parameters and the design of a method. We first attempt to predict the best timing and control its actuation behavior for debris removal operations by real-time monitoring of the machining curve changes.

Due to the highly coupled and complex non-linear relationship between the discharge parameters (included electronic and non-electric parameters) and the machining efficiency in the EDM process, it is difficult to establish a general numerical simulation model for selecting the best machining parameters [26]. Recently, AI technologies have demonstrated their outstanding performance in various fields and are continuously emerging [27], [28]. In EDM field domain, AI technologies can effectively integrate and analyze the tacit knowledge in the EDM process to have experts' analysis ability [7]. This study uses the AI technology to learn from the on-site operator's experiences which determining the timing of debris removal from the changes of the machining curve on machine screen to establish a predicted model of debris removal. During the machining process, the MRR value changes due to debris accumulation. Because MRR is not constant, the total machining time has been taken as a productivity indicator of MRR and process stability [29]. For this reason, this study adopts machining time as the performance measure of the proposed intelligent system.

III. INTELLIGENT IMPROVING EDM EFFICIENCY SYSTEM

The framework of a proposed intelligent system for improving EDM efficiency is shown in Figure 1, where the solid and dotted lines are training and testing flows. After capturing the streaming images of the machining curve in the machine screen, a feature extraction method is proposed to distinguish the carbon deposition phenomenon from the machining process effectively. The extracted features will then be fed into the ANN model to establish a debris removal predicted model. Finally, we integrate the trained model on the EDM machine to monitor and control the debris removal operation in real-time.

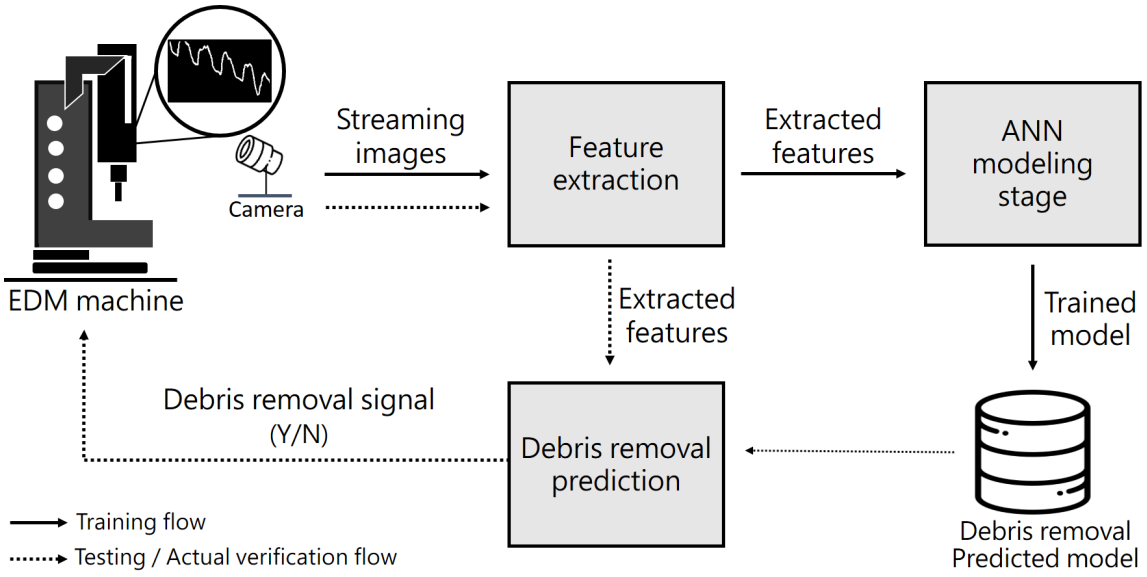

FIGURE 1. The framework of the proposed intelligent system with adaptive control of debris removal operations.

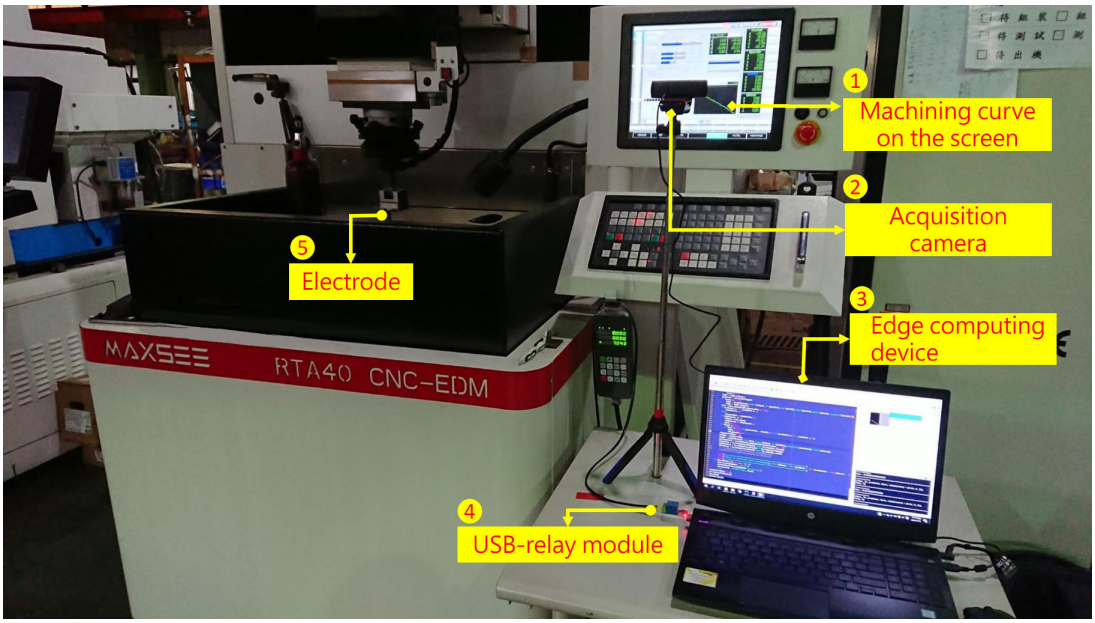

FIGURE 2. The experimental equipment layout of the EDM machine in this study.

A. EXPERIMENTAL SETUP AND DESCRIPTION

The type of EDM machine used in this research is cavity type EDM (MAXSEE RTA40). The electrode tool's size is 15 mm × 2 mm; its material used is copper alloy. The workpiece's material is tool steel (SKD11), which is a kind of high-carbon alloy steel with high hardness, high strength, and wear resistance. A schematic diagram of the experimental setup in this study is shown in Figure 2. Set up an imaging camera (Logitech C920r HD Pro) outside the EDM machine, as shown by mark ② in Figure 2, to capture the machining curve image in machine screen (mark ① in Figure 2) and send it to the edge computing device (mark ③ in Figure 2) for real-time analysis. Finally, the predicted result of whether to perform the debris removal operation is sent to the machine controller through the relay module (mark ④ in Figure 2). Mark ⑤ in Figure 2 is the electrode tool in the EDM machine. Figure 3 is a close-up view of the machining curves based on different machining conditions in the machine screen (mark ① in Figure 2). The X-axis represents the machining time, and the Y-axis can be regarded as the machining depth, the deeper of machining depth as machining time goes on. To display the EDM operation status in real-time, the machine screen

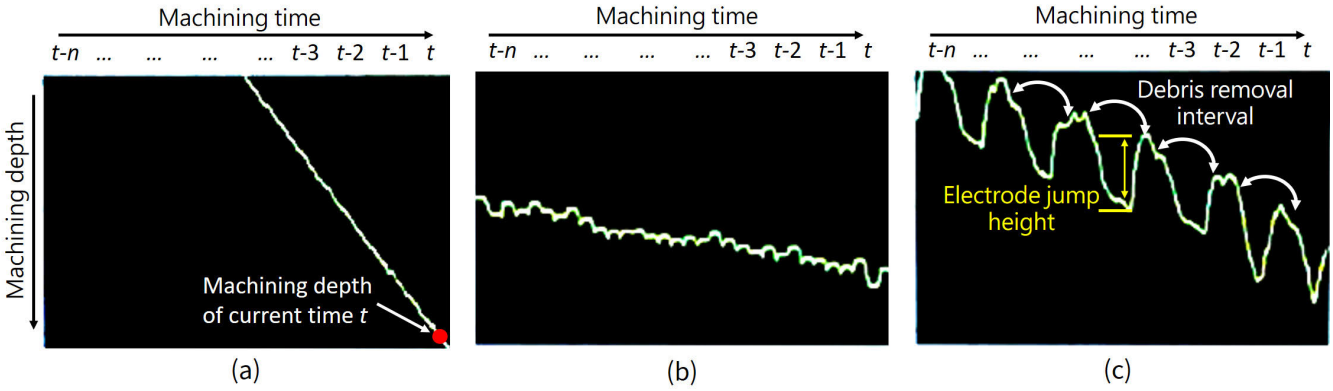

FIGURE 3. Machining curves of different machining conditions in the EDM process. (a) Good machining efficiency; (b) Poor machining efficiency (caused by carbon deposition); (c) EDM process with the preset debris removal parameter.

is updated 10 times per second. The slope of the machining curve can be regarded as an indication of measuring EDM efficiency. The higher the slope, the larger the MRR per unit time, as shown in Figure 3(a). If the debris removal operation has not been performed for a period of time in the EDM process, it will cause carbon deposition to affect machining efficiency, as shown in Figure 3(b). It can be seen from the machining curve in Figure 3(b) that the current machining efficiency is not good because the slope of the machining curve is low and tends to be flat. The machining curve in Figure 3(c) shows that the current EDM process is undergoing periodic debris removal operations. Each time the debris is removed, the machining curve will show oscillation due to electrode jump. It is worth noting that the more the number of debris removal operations, the less work time. The machining parameters of the EDM machine are set according to the general working environment of semi-finished machining (between rough and fine machining). During the machining process, the preset debris removal parameter is performed every 0.4 seconds, and the electrode jump height is set to 8mm. The detailed operation parameter settings are shown in Table 2. To avoid missing the machining status during the EDM process, the captured frequency of machining curve image is 20 times per second. The size of the captured image is 60×50 pixels.

B. FEATURE EXTRACTION

To convert the machining curve image into a binary image for subsequent feature extraction, this research first adopted the gray-level thresholding method [30] to determine the threshold value for obtaining the best binarization result automatically. Then, skeleton method in image morphology [31] will be applied to thin the machining curve into a width of 1 pixel. Let $f(x_i, y_j)$ is pixel value at any point in the image, where $i \in \{1, 2, \ldots, m\}$, $j \in \{1, 2, \ldots, n\}$, the variables m, n, are the width and height of the image, respectively. Any point (x_i, y_j) on the machining curve is $f(x_i, y_j) = 1$, it regards as foreground; otherwise, it belongs to the background

TABLE 2. The machining parameters during the EDM process used in this experiment.

Machining parameters	Values
Pulse on time	280μs
Pulse off time	50μs
Current	12A
Feed rate	400%
Work time	0.4s
Electrode jump height	8mm

($f(x_i, y_j) = 0$). The point (x_i, y_j) on the machining curve can be represented as the position y_j of the electrode tool at time point x_i. To effectively identify the states of the machining curves in the EDM machine screen, this study proposes the following 11 features, $\boldsymbol{f} = (f_1, f_2, f_3, f_4, f_5, f_6, f_7, f_8, f_9, f_{10}, f_{11})$:

- f_1: The slope of the machining curve

To calculate the slope of the straight line passing through the curve by using the linear regression method [32], [33]. This straight-line satisfies the minimum sum of the distances from each point on all the curves to the straight line. Figure 4 shows the result of applying the linear regression equation to the machining curve.

To obtain the slope of the regression equation of the machining curve, let $\hat{y}_i = \hat{\beta}_0 + \hat{\beta}_1 x_i$ be the predicted value of the machining depth at the time i, and residual $e_i = y_i - \hat{y}_i$ represents the difference between the actual value y_i and the predicted value $\hat{y}_i$ at the time i by the liner model. In the regression equation, $\hat{\beta}_0$ is the intercept, and $\hat{\beta}_1$ is the slope. The residual sum of squares (RSS) can be defined as follows [32]:

$$RSS = e_1^2 + e_2^2 + \ldots + e_n^2, \tag{1}$$

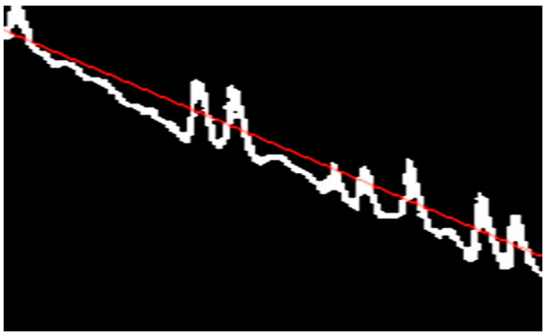

FIGURE 4. Illustration of a linear regression line through the machining curve.

the above equation can be equivalent as

$$RSS = \left(\hat{y}_1 - \hat{\beta}_0 + \hat{\beta}_1 x_1\right)^2 + \left(\hat{y}_2 - \hat{\beta}_0 + \hat{\beta}_1 x_2\right)^2 + \ldots + \left(\hat{y}_n - \hat{\beta}_0 + \hat{\beta}_1 x_n\right)^2. \quad (2)$$

To choose $\hat{\beta}_0$ and $\hat{\beta}_1$ for minimizing the RSS by using the following least squares approach [32]:

$$\hat{\beta}_1 = \frac{\sum_{i=1}^{n} (x_i - \bar{x})(y_i - \bar{y})}{\sum_{i=1}^{n} (x_i - \bar{x})^2}, \quad (3)$$

$$\hat{\beta}_0 = \bar{y} - \hat{\beta}_1 \bar{x}, \quad (4)$$

where $\bar{y} = \frac{1}{n}\sum_{i=1}^{n} y_i$ and $\bar{x} = \frac{1}{n}\sum_{i=1}^{n} x_i$ are the average values of x and y coordinates of all sample points on the machining curve, respectively. According to our observation, the higher the slope, the deeper the processing depth per unit time, and the better the EDM efficiency.

- f_2: The total number of oscillations

In general, the more frequent the debris removal operations, the worse the machining efficiency. Based on our observation, the debris removal operations during the EDM process can be characterized by the machining curve's oscillating segments. Figure 5 explains how this research automatically detects the debris removal operation from the machining curve. Figure 5(a) is the original machining curve captured from the EDM machine screen. After applying morphological thinning, the machining curve with a thickness of one pixel can be obtained. Figure 5(b) shows the line segments of interest (two oscillation segments) located in the red line area in Figure 5(a). Figure 5(c) shows the pixels' coordinates for the two oscillation segments of interest in Figure 5(b).

To detect each oscillation segment from the machining curve, we first calculate the first-order derivative of y-coordinates on the machining curve. Figure 5(d) shows the result after the first-order derivative, y', which is defined as follows:

$$y' = \frac{\partial f}{\partial x} = f(x+1) - f(x), \quad (5)$$

where $f(x+1)$ and $f(x)$ can be expressed as different machining depths of two adjacent time points, respectively. At the electrical discharge, the values of the elements in the y' vector will be positive due to machining depth deeper as machining time goes on. When removing the debris, the y values in the machining curve gradually decrease due to the electrode being raised. Meanwhile, the values of the elements in the y' vector is negative. To scan y' vector from left to right, when an element (O_{start}) is located at the junction from positive to negative values, the element is the oscillation starting point. On the contrary, an element (O_{crest}) is located at the junction from negative to positive values; it is the oscillation crest point, which means that the electrode is raised to the highest point. Repeat the above steps until the last element in y' vector. We can obtain the total number of oscillations by counting the number of O_{start} in the machining curve.

- f_3: The maximum amplitude value

The proposed maximum amplitude value on the machining curve is defined as follows:

$$O_{AMP\_max} = \max\left(O_{AMP_i}\right), \quad (6)$$

where O_{AMP_i} represents the amplitude value of ith oscillation on the machining curve, which is defined as the difference of y values for the O_{start} and O_{crest} in Figure 5(b), and N is the total number of oscillations on the machining curve.

- f_4: The average amplitude value

The proposed average amplitude value is defined as follows:

$$O_{AMP\_avg} = \frac{\sum_{i=1}^{N} O_{AMP_i}}{N}. \quad (7)$$

- f_5: The standard deviation of amplitude values

The proposed amplitude standard deviation is defined as follows:

$$O_{AMP\_std} = \sqrt{\frac{\sum_{i=1}^{N} (O_{AMP_i} - O_{AMP\_avg})^2}{N}}. \quad (8)$$

- f_6: Oscillation density

To measure the proportion of time spent on debris removal operations within a specific machining time. The feature of the oscillation density is defined as:

$$O_{density} = \frac{\sum_{i=1}^{N} O_{width_i}}{L}, \quad (9)$$

where L is the width of the image, O_{width_i} is the width of the i-th oscillation on the machining curve, which is defined as the difference for x values for the O_{crest} and O_{start}, as shown in Figure 5(b).

- f_7: The total number of oscillations belongs to the amplitude height of Category 1

Generally speaking, the deeper the machining depth, the more serious the carbon deposition. If the electrode jump height is not adjusted in time, the machining efficiency will be affected. In the following feature extraction, we roughly divide the machining situation into five categories by distinguishing the oscillation amplitude height in the machining

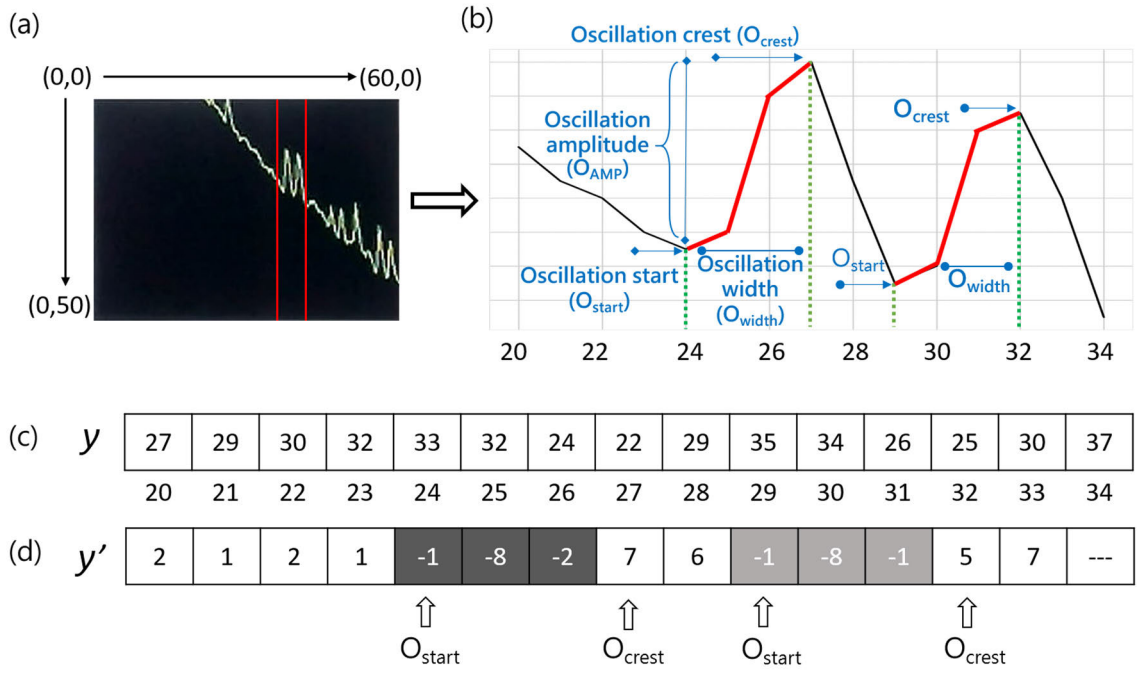

FIGURE 5. Graphically illustrate the status of debris removal operation in the machining curve. (a) Original machining curve; (b) Two oscillation segments located in the red line area in Figure 5(a); (c) The pixels' coordinates for the two oscillation regions in Figure 5(b); (d) The first-order derivative of y-coordinates on the machining curve.

curve. The total number of oscillations belongs to the amplitude height of Category 1 is defined as:

$$f_7 = \text{Card}\left\{ \begin{matrix} \text{O}_{\text{AMP}_i} | \text{O}_{\text{AMP}_i} \leq 0.1 \times H, \\ i \in \{1, 2, \ldots, N\} \end{matrix} \right\}, \tag{10}$$

where H is the height of the image, Card$\{\cdot\}$ is a set function, which returns the number of qualified ones.

- f_8: The total number of oscillations belongs to the amplitude height of Category 2

$$f_8 = \text{Card}\left\{ \begin{matrix} \text{O}_{\text{AMP}_i} | 0.1 \times H < \text{O}_{\text{AMP}_i} \leq 0.2 \times H, \\ i \in \{1, 2, \ldots, N\} \end{matrix} \right\}. \tag{11}$$

- f_9: The total number of oscillations belongs to the amplitude height of Category 3

$$f_9 = \text{Card}\left\{ \begin{matrix} \text{O}_{\text{AMP}_i} | 0.2 \times H < \text{O}_{\text{AMP}_i} \leq 0.3 \times H, \\ i \in \{1, 2, \ldots, N\} \end{matrix} \right\}. \tag{12}$$

- f_{10}: The total number of oscillations belongs to the amplitude height of Category 4

$$f_{10} = \text{Card}\left\{ \begin{matrix} \text{O}_{\text{AMP}_i} | 0.3 \times H < \text{O}_{\text{AMP}_i} \leq 0.4 \times H, \\ i \in \{1, 2, \ldots, N\} \end{matrix} \right\}. \tag{13}$$

- f_{11}: The total number of oscillations belongs to the amplitude height of Category 5

$$f_{11} = \text{Card}\left\{ \begin{matrix} \text{O}_{\text{AMP}_i} | \text{O}_{\text{AMP}_i} > 0.4 \times H, \\ i \in \{1, 2, \ldots, N\} \end{matrix} \right\}. \tag{14}$$

IV. CLASSIFICATION

Deep learning has recently become a trendy research topic in the AI field [27], [28], [34], [35]; it solves the core problems in representation learning by expressing simpler representations, thereby enabling computers to construct complex concepts from simpler concepts [36]. Generally speaking, a deep neural network is one kind of ANN network architecture; it refers to a feedforward neural network with more than one hidden layer. Each hidden layer has several neurons. Each neuron takes all the lower layer output as input, then multiplies them by the weight vector, sums the results, and then passes it to the next layer neuron through a non-linear activation function such as sigmoid, tanh, or rectified linear units (ReLU). The formula can be expressed as follows [37]:

$$z_i^{(k)} = g\left(w_{0,i}^{(k)} + \sum_{j=1}^{n} z_j^{(k-1)} w_{j,i}^{(k)} \right), \tag{15}$$

where $z_i^{(k)}$ denotes the output neuron of the i-th neuron in the k-th layer, $w_{0,i}^{(k)}$ is a bias added to the i-th neuron, n is the total number of neurons at the $k-1$ layer, $w_{j,i}^{(k)}$ denotes the

connecting weight from the j-th neuron in the $k-1$ layer to the i-th neuron in the k layer, and $g(\cdot)$ a non-linear activation function. In this study, we adopt the ReLU function, because the ReLU function can effectively overcome deficiencies of gradient disappearance and slow convergence in the training process [35]. The above expression can be represented in the following vector form for simplicity of notation:

$$z_i^{(k)} = g\left(\mathbf{z}^{(k-1)} \cdot \mathbf{w}_i^{(k)}\right). \tag{16}$$

The bias term of the above expression is integrated into the column weight vector $\mathbf{w}_i^{(k)}$, and the vector $\mathbf{z}^{(k-1)}$ extra expands dimension of 1 for the computation. In ANN architecture, the first layer is the input layer, and the last layer is the output layer. Finally, this study applies the softmax function to compute the final classification probabilities as the output result in the last layer [38]:

$$y_i = \frac{\exp(z_i^{(L)})}{\sum_j \exp(z_j^{(L)})}, \tag{17}$$

where L is the last layer, $z_i^{(L)}$ is computed as $z_i^{(L)} = \mathbf{z}^{(L-1)} \cdot \mathbf{w}_i^{(L)}$. To further improve the performance of classification, the training process uses the back-propagation algorithm to minimize the loss function, which can be expressed as [39]

$$D = \frac{1}{2N} \sum_{m=1}^{N} \left\| \hat{y}_m - y_m \right\|^2, \tag{18}$$

where N is the total number of training samples, and $\hat{y}_m$ and y_m represent the actual and predicted values of whether the debris removal operation should be carried out for training sample m, respectively. The ANN model architecture used in this paper is shown in Figure 6.

This study only extracted 11 features from a machining curve image as input neurons of ANN, instead of common deep learning architectures, such as the convolutional neural networks (CNNs), which consider the entire image at the input layer. Therefore, the adopted method is more suitable for application in a manufacturing site with low computing resources.

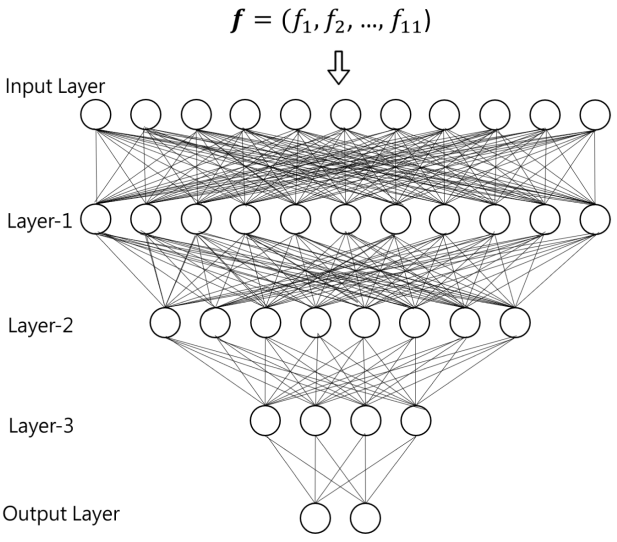

FIGURE 6. The proposed ANN model architecture.

V. EXPERIMENTAL RESULTS AND DISCUSSION

The experiment in this study is divided into two stages. The first stage is to test the effectiveness of the proposed feature set ($\boldsymbol{f} = (f_1, f_2, \ldots, f_{11})$) in debris removal prediction using the ANN model, and the second stage is to verify the effectiveness of the proposed intelligent system in improving machining efficiency. In the acquisition of experimental data, this study collected 3,744 machining curve images from the machine screen during the EDM process, of which 80% (2994) were used as the training dataset, and the remaining 20% (750) were used as the testing dataset. All images in this experiment are marked in two different classes by the on-site senior EDM technician based on their experiences: no need for debris removal (high machining efficiency) and need for debris removal (low machining efficiency). Table 3 shows the used number of images for different machining states in training and testing datasets, respectively.

TABLE 3. Description of experimental datasets.

Dataset	Training datasets	Testing datasets
No need for debris removal	1476	375
Need for debris removal	1518	375
	2994	750

To quantitatively evaluate the effectiveness of the feature set proposed in this study, the following three measurements are adopted, including accuracy, precision, and recall. As shown in Table 4, let TP, TN, FP, and FN represent "true positive", "true negative", "false positive", and "false negative", respectively, in the confusion matrix. In this study, we regard the need for debris removal as a positive condition and the no need for debris removal as a negative condition. The definitions for the above three measurements are listed below [40]:

$$\text{Precision} = \text{TP}/(\text{TP} + \text{FP}), \tag{19}$$

$$\text{Recall} = \text{TP}/(\text{TP} + \text{FN}), \tag{20}$$

$$\text{Accuracy} = (\text{TP} + \text{TN})/(\text{TP} + \text{TN} + \text{FP} + \text{FN}). \tag{21}$$

Precision, also known as precision rate, is the proportion of all the test results of the need for debris removal that truly needs debris removal. Recall, also known as a true positive

TABLE 4. Cross-relations between test and actual results.

Confusion matrix (P: positive; N: negative)		Actual results P	Actual results N
Test results	P	TP	FP
	N	FN	TN

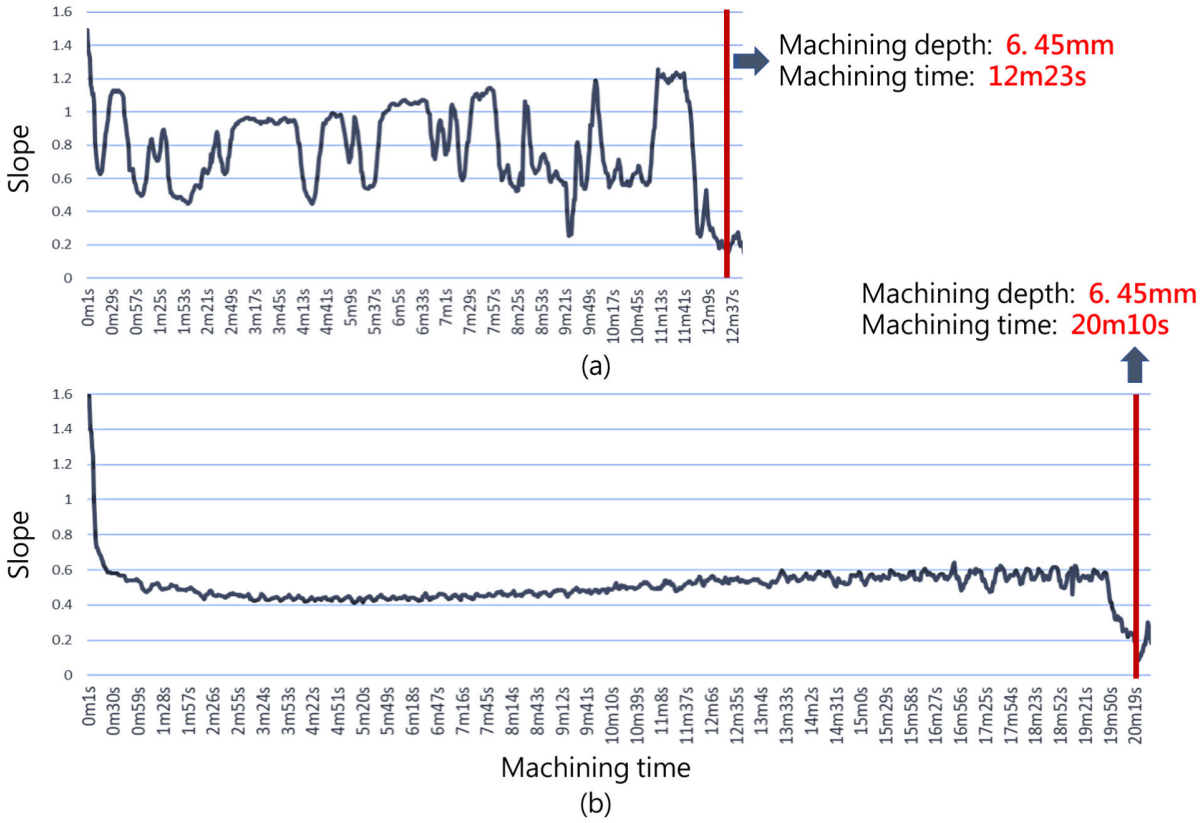

FIGURE 7. A comparison of the proposed intelligent system and used the preset debris removal frequency in the EDM efficiency. (a) Used the proposed intelligent system; (b) Used the preset debris removal parameter.

rate (TPR), represents the proportion of all the actual results of the need for debris removal that truly needs debris removal. The accuracy is the proportion of both true need for and true not need for debris removal in all test results. It is the overall correct classification rate of all test results.

After analysis of our experimental results, the TP, TN, FP, and FN are 357, 370, 18, and 5, respectively. The accuracy is 96.93% ((357 + 370)/750), and the results of precision and recall are 95.20% (357/(357 + 18)) and 98.62% (357/(357 + 5)), respectively. To further evaluate the effectiveness of the proposed feature set, the testing samples will be tested against using logistic regression (LR) [41], random forest (RF) [42], and support vector machine (SVM) classifiers [43], respectively, to estimate accuracy. It can be seen from Table 5 that the ANN model architecture used in this paper is not much different from other classifiers in the accuracy evaluation. Under the test of different classifiers, the proposed feature set still can maintain a certain accuracy, which shows that the proposed feature set is discriminative in debris removal prediction. Used other types of deep neural networks [44], [45] or some advanced classifiers [46] may improve classification performance, but this is beyond the scope of this paper.

In addition to verifying the classification performance of the proposed feature set, in the second stage of the

TABLE 5. Comparisons of accuracy for the proposed feature set using different classifiers.

Classifier	LR	RF	SVM	ANN
Accuracy	95.60%	95.86%	95.20%	96.93%

experiment, this paper integrates the established debris removal predicted model into the EDM machine for verifying the effectiveness of the proposed intelligent system in improving machining efficiency. The proposed intelligent improving EDM efficiency system could autonomously determine the timing of debris removal from the real-time streaming machining images under the machining conditions mentioned in Table 2. Once the system decides to perform the debris removal operation, the edge computing device will send a debris removal signal to the machine controller through the relay module to trigger the electrode jump event. The proposed system will only send a debris removal signal in a low machining efficiency state (debris accumulation impact). Therefore, the proposed system dramatically reduces unnecessary debris removal operations to improve machining efficiency.

Figure 7 shows a comparison in EDM efficiency between controls adaptively of debris removal operation by the

proposed intelligent system and the preset debris removal parameter. The X-axis and Y-axis in Figure 7 are machining time and the slope of the machining curve, respectively. Remember that the higher the slope, the larger the MRR per unit time, the better the machining efficiency. In most cases in Figure 7(b), the slope is less than 0.6. The reason is that too many debris removal operations will result in low machining efficiency. It takes 20 minutes and 10 seconds to reach a machining depth of 6.45mm for the workpiece made of tool steel as we use preset the debris removal parameter. On the contrary, the proposed intelligent system only takes 12 minutes and 23 seconds to reach the same machining depth, as shown in Figure 7(a). The proposed intelligent system could save nearly 38.60% ($\frac{1210-743}{1210} \times 100$) of machining time for the machining depth of 6.45mm under specific EDM conditions.

VI. CONCLUSION

This paper has successfully developed an intelligent system for improving the EDM efficiency, which autonomously determines debris removal operations by the established debris removal predicted model instead of using the preset debris removal parameter. To achieve the purpose of this paper, we first attempt to apply AI and computer vision technologies to real-time analyze streaming images of the machining curve in machine screen to establish a debris removal predicted model. To test the effectiveness of the proposed feature set in debris removal prediction, no matter which classifier is used, such as logistic regression, random forest, and SVM, the proposed feature set performs well in classification performance. The classification result shows that the established debris removal predicted model by ANN model could achieve 96.93% accuracy for 750 machining curve images in a testing dataset. To further verify the effectiveness of machining efficiency improvement, the proposed system could save nearly 38.60% of machining time for the machining depth of 6.45mm under specific machining conditions compared to using the fixed behavior pattern of the preset debris removal parameter.

This paper shows that the debris removal frequency is one of the main factors affecting machining efficiency by analyzing the results of the complete experiment. Review the researches that EDM-related in recent years, the adaptive control of debris removal operations for non-electric parameters has not been applied to improve electric discharge machining efficiency. The findings of this paper can be applied to the actual manufacturing site and bring significant improvement in machining efficiency. The principle of electrical discharge machining is complex, and many machining parameters affect its efficiency, and the degree of mutual coupling between the parameters is very high. At present, this research only focuses on the parameter of the debris removal operation. In the future, we will consider more machining parameters at the same time, such as sparking gap, jump height, pulse off-time, etc., to develop a next-generation intelligent EDM machine.

REFERENCES

[1] K. H. Ho and S. T. Newman, "State of the art electrical discharge machining (EDM)," *Int. J. Mach. Tools Manuf.*, vol. 43, no. 13, pp. 1287–1300, Oct. 2003.

[2] M. A. Norliana, D. G. Solomon, and M. F. Bahari, "A review on current research trends in electrical discharge machining," *Int. J. Mach. Tools Manufact.*, vol. 47, pp. 1214–1228, Jun. 2007.

[3] M. Gangil, M. K. Pradhan, and R. Purohit, "Review on modelling and optimization of electrical discharge machining process using modern techniques," *Mater. Today, Process.*, vol. 4, no. 2, pp. 2048–2057, 2017.

[4] C. J. Luis, I. Puertas, and G. Villa, "Material removal rate and electrode wear study on the EDM of silicon carbide," *J. Mater. Process. Technol.*, vols. 164–165, pp. 889–896, May 2005.

[5] P. Sadagopan and B. Mouliprasanth, "Investigation on the influence of different types of dielectrics in electrical discharge machining," *Int. J. Adv. Manuf. Technol.*, vol. 92, nos. 1–4, pp. 277–291, Sep. 2017.

[6] J. Anitha, R. Das, and M. K. Pradhan, "Multi-objective optimization of electrical discharge machining processes using artificial neural network," *Jordan J. Mech. Ind. Eng.*, vol. 1, pp. 11–18, May 2016.

[7] C. Fenggou and Y. Dayong, "The study of high efficiency and intelligent optimization system in EDM sinking process," *J. Mater. Process. Technol.*, vol. 149, nos. 1–3, pp. 83–87, Jun. 2004.

[8] K. Salonitis, A. Stournaras, P. Stavropoulos, and G. Chryssolouris, "Thermal modeling of the material removal rate and surface roughness for die-sinking EDM," *Int. J. Adv. Manuf. Technol.*, vol. 40, nos. 3–4, pp. 316–323, Jan. 2009.

[9] S. N. Joshi and S. S. Pande, "Development of an intelligent process model for EDM," *Int. J. Adv. Manuf. Technol.*, vol. 45, nos. 3–4, pp. 300–317, Nov. 2009.

[10] T. Rajmohan, R. Prabhu, G. S. Rao, and K. Palanikumar, "Optimization of machining parameters in electrical discharge machining (EDM) of 304 stainless steel," *Procedia Eng.*, vol. 38, pp. 1030–1036, Jan. 2012.

[11] K. P. Maity and M. Choubey, "A review on vibration-assisted EDM, micro-EDM and WEDM," *Surf. Rev. Lett.*, vol. 26, no. 05, Jun. 2019, Art. no. 1830008.

[12] H.-P. Nguyen and V.-D. Pham, "Single objective optimization of die- sinking electrical discharge machining with low frequency vibration assigned on workpiece by taguchi method," *J. King Saud Univ.-Eng. Sci.*, vol. 33, no. 1, pp. 37–42, Jan. 2021.

[13] X. Wang, Z. Liu, R. Xue, Z. Tian, and Y. Huang, "Research on the influence of dielectric characteristics on EDM of titanium alloy," *Int. J. Adv. Manuf. Technol.*, vol. 72, pp. 979–987, Jun. 2014.

[14] Y. Margrab, H. Chang, W. Zhang, F. Ma, Z. Sha, and S. Zhang, "A simulation study of debris removal process in ultrasonic vibration assisted electrical discharge machining (EDM) of deep holes," *Micromachines*, vol. 9, no. 8, pp. 1–22, 2018.

[15] E. B. Margrab, S. K. Gupta, F. P. McCluskey, and P. A. Sandborn, *Integrated Product and Process Design and Development-The Product Realization Process*, 2th ed. New York, NY, USA: CRC Press, 2010.

[16] S. Cetin, A. Okada, and Y. Uno, "Effect of debris distribution on wall concavity in deep-hole EDM," *JSME Int. J. Ser. C Mech. Syst.*, vol. 47, no. 2, pp. 553–559, 2004.

[17] J. Wang and F. Han, "Simulation model of debris and bubble movement in consecutive-pulse discharge of electrical discharge machining," *Int. J. Mach. Tools Manuf.*, vol. 77, pp. 56–65, Feb. 2014.

[18] J. Wang and F. Han, "Simulation model of debris and bubble movement in electrode jump of electrical discharge machining," *Int. J. Adv. Manuf. Technol.*, vol. 74, nos. 5–8, pp. 591–598, Sep. 2014.

[19] J. Wang and Z. Jia, "Efficiency improvement in electrical discharge machining (EDM) of constant section cavity based on experimental study and numerical calculations," *Prod. Eng.*, vol. 12, pp. 567–579, May 2018.

[20] B. Nahak and A. Gupta, "A review on optimization of machining performances and recent developments in electro discharge machining," *Manuf. Rev.*, vol. 6, p. 2, Feb. 2019.

[21] T. Muthuramalingam and B. Mohanb, "A review on influence of electrical process parameters in EDM process," *Arch. Civil Mech. Eng.*, vol. 15, no. 1, pp. 89–94, 2015.

[22] M. Hanif, W. Ahmad, S. Hussain, M. Jahanzaib, and A. H. Shah, "Investigating the effects of electric discharge machining parameters on material removal rate and surface roughness on AISI D2 steel using RSM-GRA integrated approach," *Int. J. Adv. Manuf. Technol.*, vol. 101, nos. 5–8, pp. 1255–1265, Apr. 2019.

[23] S. A. Mastud, N. S. Kothari, R. K. Singh, and S. S. Joshi, "Modeling debris motion in vibration assisted reverse micro electrical discharge machining process (R-MEDM)," *J. Microelectromech. Syst.*, vol. 24, no. 3, pp. 661–676, Jun. 2015.
[24] G. Zhu, M. Zhang, Q. Zhang, Z. Song, and K. Wang, "Machining behaviors of vibration-assisted electrical arc machining of W9Mo3Cr4 V," *Int. J. Adv. Manuf. Technol.*, vol. 96, nos. 1–4, pp. 1073–1080, Apr. 2018.
[25] Y. Liu, H. Chang, W. Zhang, F. Ma, Z. Sha, and S. Zhang, "A simulation study of debris removal process in ultrasonic vibration assisted electrical discharge machining (EDM) of deep holes?" *Micromachines*, vol. 9, no. 8, pp. 1–22, 2018.
[26] S. N. Joshi and S. S. Pande, "Intelligent process modeling and optimization of die-sinking electric discharge machining," *Appl. Soft Comput.*, vol. 11, no. 2, pp. 2743–2755, Mar. 2011.
[27] C.-H. Lee, J.-S. Jwo, H.-Y. Hsieh, and C.-S. Lin, "An intelligent system for grinding wheel condition monitoring based on machining sound and deep learning," *IEEE Access*, vol. 8, pp. 58279–58289, 2020.
[28] J. S. Jwo, C. S. Lin, and C. H. Lee, "Smart technology–driven aspects for human-in-the-loop smart manufacturing," *Int. J. Adv. Manuf. Technol.*, vol. 114, pp. 1741–1752, May 2021.
[29] I. Ayesta, B. Izquierdo, J. A. Sánchez, J. M. Ramos, S. Plaza, I. Pombo, N. Ortega, H. Bravo, R. Fradejas, and I. Zamakona, "Influence of EDM parameters on slot machining in C1023 aeronautical alloy," *Procedia CIRP*, vol. 6, pp. 129–134, Mar. 013.
[30] N. Otsu, "A threshold selection method from gray-level histograms," *IEEE Trans. Syst., Man, Cybern.*, vol. SMC-9, no. 1, pp. 62–66, Jan. 1979.
[31] R. C. Gonzales and R. E. Wood,*Digital Image Processing*. Upper Saddle River, NJ, USA: Pearson, 2018, pp. 710–722.
[32] G. James, D. Written, T. Hastie, and R. Tibshirani, *An Introduction to Statistical Learning with Applications*. New York, NY, USA: Springer, 2013.
[33] M. J. Zaki, *Data Mining and Machine Learning: Fundamental Concepts and Algorithms*. Cambridge, U.K.: Cambridge Univ. Press, 2020.
[34] N. N. An, N. Q. Thanh, and Y. Liu, "Deep CNNs with self-attention for speaker identification," *IEEE Access*, vol. 7, pp. 85327–85337, 2019.
[35] Z. Huang, J. Zhu, J. Lei, X. Li, and F. Tian, "Tool wear predicting based on multi-domain feature fusion by deep convolutional neural network in milling operations," *J. Intell. Manuf.*, vol. 4, pp. 1–14, Aug. 2019.
[36] I. Goodfellow, Y. Bengio, and A. Courville, *Deep Learning*. Cambridge, MA, USA: MIT Press, 2016.
[37] O. Abdel-Hamid, A. R. Mohamed, H. Jiang, L. Deng, G. Penn, and D. Yu, "Convolutional neural networks for speech recognition," in *IEEE/ACM Trans. Audio, Speech, Lang. Process.*, vol. 22, no. 10, pp. 1533–1545, Oct. 2014, doi: 10.1109/TASLP.2014.2339736.
[38] R. Huang, Y. Liao, S. Zhang, and W. Li, "Deep decoupling convolutional neural network for intelligent compound fault diagnosis," *IEEE Access*, vol. 7, pp. 1848–1858, 2019.
[39] R. Jiao, X. Huang, X. Ma, L. Han, and W. Tian, "A model combining stacked auto encoder and back propagation algorithm for short-term wind power forecasting," *IEEE Access*, vol. 6, pp. 17851–17858, 2018.
[40] P.-L. Lin, P.-W. Huang, C.-H. Lee, and M.-T. Wu, "Automatic classification for solitary pulmonary nodule in CT image by fractal analysis based on fractional brownian motion model," *Pattern Recognit.*, vol. 46, no. 12, pp. 3279–3287, Dec. 2013.
[41] H. Li, Y. Wang, P. Zhao, X. Zhang, and P. Zhou, "Cutting tool operational reliability prediction based on acoustic emission and logistic regression model," *J. Intell. Manuf.*, vol. 26, no. 5, pp. 923–931, Oct. 2015.
[42] D. Wu, C. Jennings, J. Terpenny, R. X. Gao, and S. Kumara, "A comparative study on machine learning algorithms for smart manufacturing: Tool wear prediction using random forests," *J. Manuf. Sci. Eng.*, vol. 139, no. 7, Jul. 2017.
[43] D. Shi and N. N. Gindy, "Tool wear predictive model based on least squares support vector machines," *Mech. Syst. Signal Process.*, vol. 21, no. 4, pp. 1799–1814, May 2007.
[44] M. Nilashi, H. Ahmadi, A. Sheikhtaheri, R. Naemi, R. Alotaibi, A. A. Alarood, A. Munshi, T. A. Rashid, and J. Zhao, "Remote tracking of Parkinson's disease progression using ensembles of deep belief network and self-organizing map," *Expert Syst. Appl.*, vol. 159, Nov. 2020, Art. no. 113562.
[45] S. Chhetri, A. Alsadoon, T. Al-Dala'in, P. W. C. Prasad, T. A. Rashid, and A. Maag, "Deep learning for vision-based fall detection system: Enhanced optical dynamic flow," *Comput. Intell.*, vol. 37, no. 1, pp. 578–595, Feb. 2021.
[46] T. Rashid, U. of Kurdistan Hewler, S. Abdullah, and K. University, "A hybrid of artificial bee colony, genetic algorithm, and neural network for diabetic mellitus diagnosing," *ARO-Sci. J. Koya Univ.*, vol. 6, no. 1, pp. 55–64, Jun. 2018.

CHENG-HSIUNG LEE received the B.I.M. and M.I.M. degrees in information management from the Chaoyang University of Technology, in 2002 and 2004, respectively, and the Ph.D. degree in computer science and engineering from National Chung-Hsing University, Taichung, Taiwan, in 2013.

From September 2017 to July 2018, he was a Postdoctoral Research Fellow with the Center of Intelligent and Innovation Manufacturing System, Tunghai University, Taiwan. He is currently an Assistant Professor with the Master Program of Digital Innovation, Tunghai University. His current research interests include artificial intelligence, big data analytics, computer vision, and smart manufacturing.

TON-SHIN LAI received the E.M.B.A. degree in executive master of business administration from Tunghai University, Taichung, Taiwan, in 2021. He is currently pursuing the master's degree with the Master Program of Digital Innovation, Tunghai University. He is the Chairman of MAXSEE Industry Company Ltd. He has been deeply involved in the manufacturing industry for more than 30 years and is committed to developing electric discharge machines and machining center machine products. His research interests include business AI, smart manufacturing, and smart machine.